J Nanostruct 15(3): 1208-1219, Summer 2025

RESEARCH PAPER

Perovskites Solar Cells Study Optimization Thickness, Temperature and Work Function

Murtadha J. Edam [1], Alaa S Mahdi [1], Samir M. AbdulAlmohsin [1], Hawraa M. Khadier [2]*

[1] *Department of Physics, College of Education for Pure Sciences, University of Thi-Qar, Thi-Qar, 64001, Iraq*

[2] *Department of Physics, College of Sciences, University of Thi-Qar, Thi-Qar, 64001, Iraq*

ARTICLE INFO

Article History:
Received 10 April 2025
Accepted 26 June 2025
Published 01 July 2025

Keywords:
Nano-scaffold perovskite solar cell
Simulator SCAPS-1D
Thin film
Work-function

ABSTRACT

The $Cs_2AgBi_{0.75}Sb_{0.25}Br_6$ based perovskite solar cell (PSC) has demonstrated a high power conversion efficiency (PCE > 16%) and exceptional air stability. A comprehensive study of the interfaces in perovskite solar cells, coupled with the optimization of many parameters, is still necessary for further enhancement in PCE. This study quantitatively analyzes lead-free $Cs_2AgBi_{0.75}Sb_{0.25}Br_6$ utilizing a solar cell capacitance simulator (SCAPS–1D). The electron transport layer (ZnO) and the hole transport layer (Cu_2O) were analyzed comparably. The work function, temperature, and thickness of the PSC layers have been meticulously examined. The results indicate that the efficiency of the device is significantly influenced by the thickness of the absorber layer. The simulation determined the maximum PCE of $Cs_2AgBi_{0.75}Sb_{0.25}Br_6$-based PSCs to be 16.23%, at thickness 0.1μm of absorber layer with an open circuit voltage (V_{oc}) of 1.3666 V, a short-circuit current density (J_{sc}) of 23.825 mA/cm², and a fill factor (FF) of 49.84%. Our exceptional results unequivocally indicate that $Cs_2AgBi_{0.75}Sb_{0.25}Br_6$- based PSCs are poised to emerge as the most efficient single-junction solar cell technology in the near future.

How to cite this article
Edam M., Mahdi A., AbdulAlmohsin S., Khadier H. Perovskites Solar Cells Study Optimization Thickness, Temperature and Work Function . J Nanostruct, 2025; 15(3):1208-1219. DOI: 10.22052/JNS.2025.03.038

INTRODUCTION

Improvements in technology, increased commercial manufacturing, and the identification of affordable materials have all contributed to solar photovoltaic (PV) technology's remarkable progress in the last several decades [1-3]. Improving solar cells' efficiency is key for commercializing this technology. This discrepancy between photon and bandgap energies causes energy loss in single-junction PV devices, which causes certain limitations. As is widely known, the bandgap energy must be equivalent to the photon energy for its efficient extraction as electric power. For photons with energies below the bandgap, absorption occurs automatically; for those with higher energies, carrier thermalization causes to lose energy, rendering them ineffective in the conduction process [4]. Although perovskite solar cells produce more light when their density is increased, the photocurrent efficiency (PCE) stays the same because of restrictions on electron length [5-7]. Perovskites made of tin halides, such as $CsSnI_3$, $MASnI_3$, and $FASnI_3$, have been studied. There is an inherent lack of stability in

* *Corresponding Author Email: murtadhaj11@utq.edu.iq*

the latter two perovskites [8, 9]. All-inorganic lead-free $CsSnI_3$ perovskite is presently the most promising contender to Pb-based light harvesting materials. Recent research have demonstrated that using cesium (Cs) instead of organic cations in perovskite structures can greatly improve thermal stability and performance in outdoor and ambient devices [10, 11]. With a PCE of 10.1%, $CsSnI_3$ was the most efficient lead-free all-inorganic PSC [12, 13]. As a potential alternative to lead halide

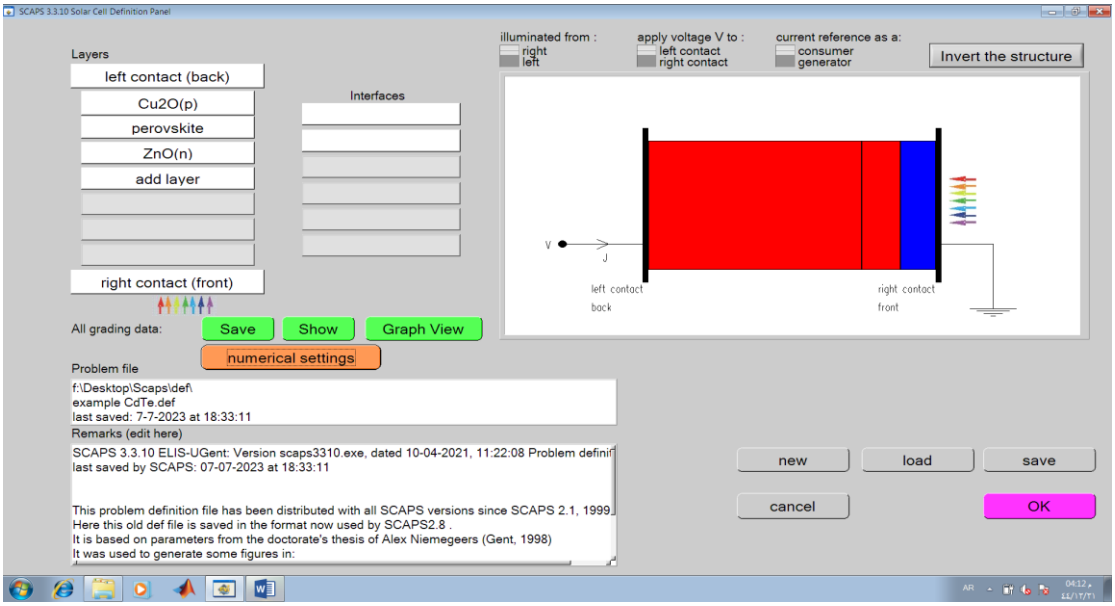

Fig. 1. Definition of $Cu_2O/Cs_2AgBi_{0.75}Sb_{0.25}Br_6/ZnO$ heterojunction solar cells in the SCAPS panel.

Table 1. Modeling fundamental parameters [2, 23-28].

Parameters	Cu_2O	$Cs_2AgBi_{0.75}Sb_{0.25}Br_6$	ZnO
Energy gap (ev)	2.170	1.800	3.3
Electron affinity (ev)	3.2	3.580	4.1
Permission of electrical	7.2	6.500	9
The density of levels for CB operating ($1/cm^2$)	2.000E+17	2.200E+19	1.000E+19
The density of levels for VB operating ($1/cm^2$)	1.100E+19	1.800E+19	1.000E+19
mobility of Electron ($cm^2/v.s$)	2E+0	2.000E+0	50
Hole mobility ($cm^2/v.s$)	8.000E+0	2.000E+0	5
Donor Concentration N_D/cm^{-3}	1.000E+7	1.000E+13	1.000+17
Acceptor Concentration N_A/cm^{-3}	1.000E+18	1.000E+17	0.000E+0

perovskites, halide double perovskites with the formula $A_2B'B''X_6$ (where A = Cs, MA; B' = Bi, Sb; B'' = Cu, Ag; and X = Cl, Br, I) have been studied [14]. The stability issues with perovskite solar cells have been successfully addressed, and this new family of materials has proven to be quite stable when subjected to various weather conditions. Although $Cs_2AgBiBr_6$ deteriorated over many weeks when exposed to both ambient air and light, McClure et al. [15] discovered that $Cs_2AgBiCl_6$ and $Cs_2AgBiBr_6$ perovskites were stable in air. There are currently no Pb-free solar cells on the market that can compete with the efficiency of Pb-containing perovskites [16]. Perovskite absorber material ($Cs_2AgBi_{0.75}Sb_{0.25}Br_6$) is suggested by Min Chen et al. [17], in terms of performance and air stability.

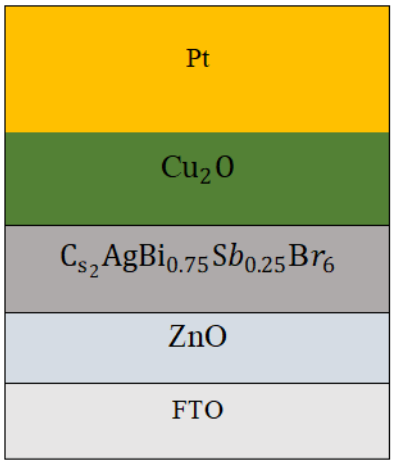

Fig. 2. Design of FTO/Cu_2O/$Cs_2AgBi_{0.75}Sb_{0.25}Br_6$/ZnO/Pt.

Table 2. The SCAPS simulation parameters.

Left contact electrical properties (Pt)	
Thermionic emission /surface recombination Velocity of electron (cm/s)	10^7
Thermionic emission /surface recombination Velocity of hole (cm/s)	10^7
Metal (Pt) work function (ev)	5.6
Right contact electrical properties	
Thermionic emission /surface recombination Velocity of electron (cm/s)	10^7
Thermionic emission /surface recombination Velocity of hole (cm/s)	10^7
work function of FTO (ev)	4.4

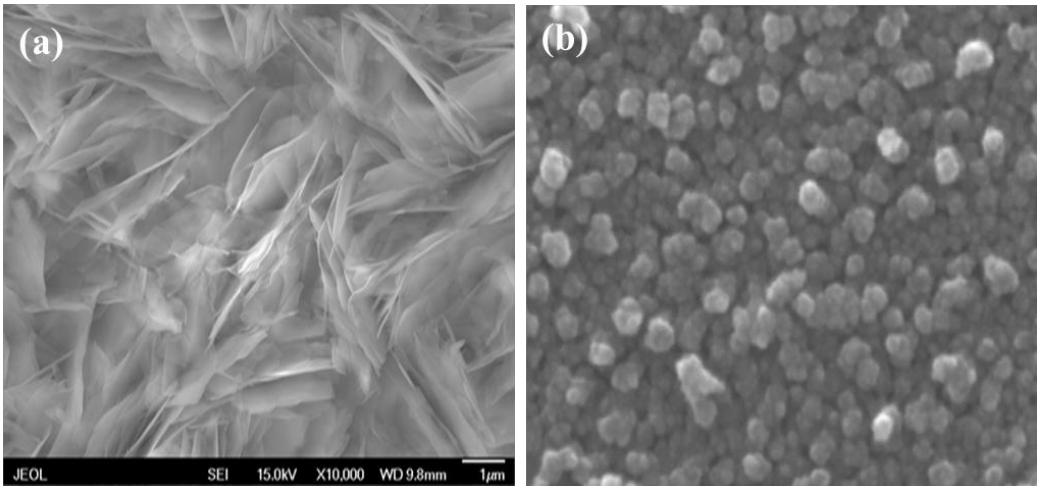

Fig. 3. SEM images of (a) ZnO nanoplate and (b) Cu_2O nanostructures.

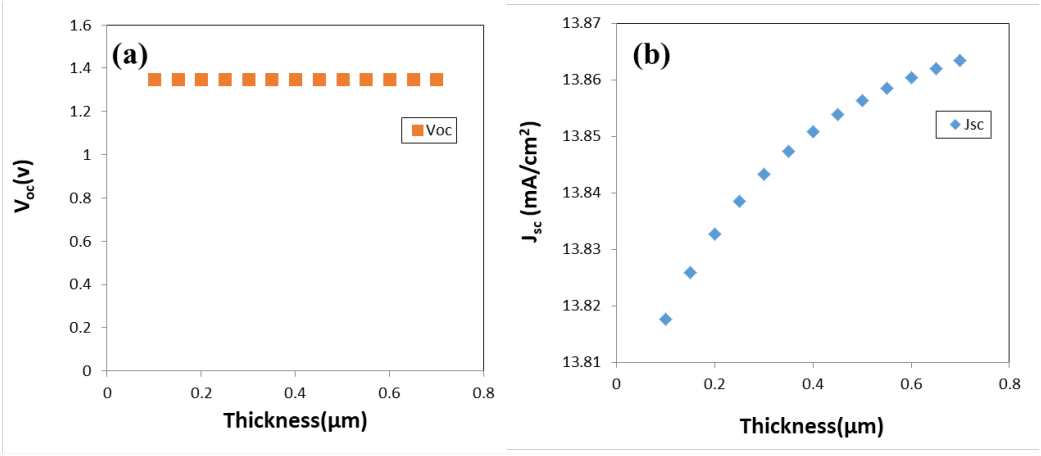

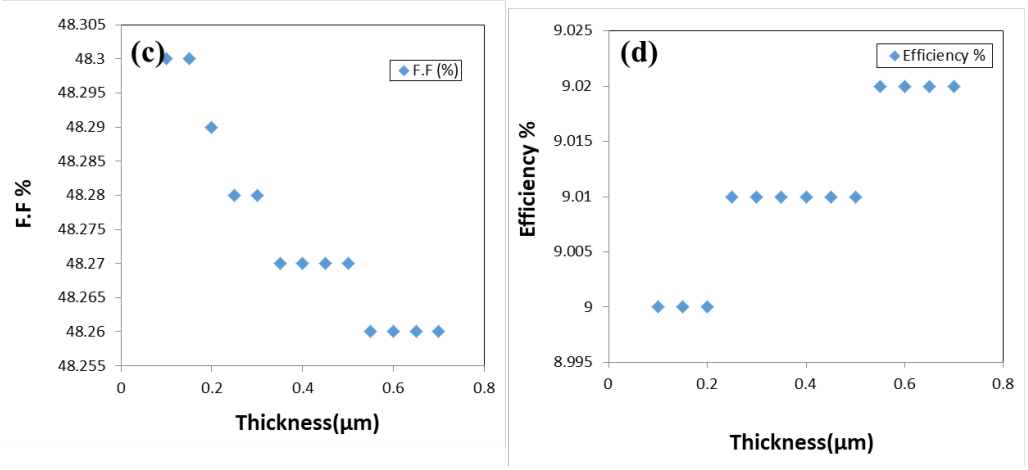

Fig. 4. The range of possibilities of (a) V_{oc}, (b) J_{sc}, (c) F.F, and (d) Efficiency with different thicknesses of Cu_2O.

A PCE of 7% is demonstrated by the device based on $Cs_2AgBi_{0.75}Sb_{0.25}Br_6$. This model was obtained using fundamental literature data provided by the corresponding simulation studies [18, 19]. The present investigation relies on a perovskite $Cs_2AgBi_{0.75}Sb_{0.25}Br_6$. This material was selected for its 1.8 eV bandgap since it has several benefits over halogenated perovskites. It is linked to a ZnO-based electron transport layer and a Cu_2O-based HTL. Since Cu_2O is inexpensive, abundant in solar energy materials, and shows interest as an inorganic HTL for PSC applications, it was chosen to serve as the HTL [20]. In standalone settings, we predicted the implications on the photovoltaic characteristics of diverse thickness of the absorbent, electron transport, and hole transit layers. We identified the optimal cell functional parameters based on the results. We also investigated the impact of the working temperature and work function on the parameters and efficiency of the solar cell [21].

MATERIALS AND METHODS

Simulating devices and characterization

One of the most important tools in this field is simulation, which may help us understand proposed physical explanation, and the effect of initial parameters on the performance of cell systems (Fig. 1 and Table 1) [2, 22-27].

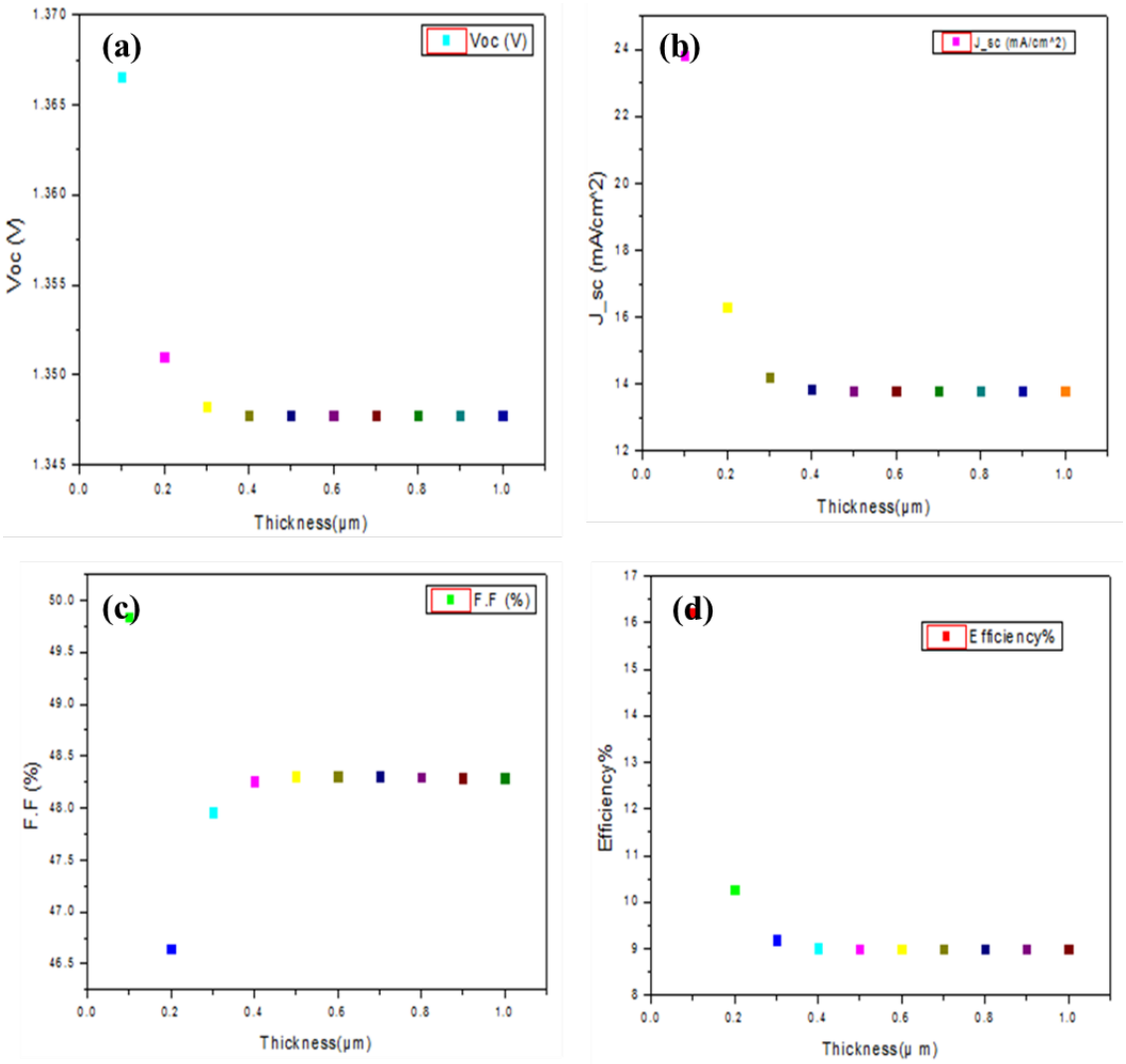

Fig. 5. Photoelectric parameters changes by $Cs_2AgBi_{0.75}Sb_{0.25}Br_6$.

Current research provides use of SCAPS for modelling perovskite solar cells based on Cu_2O/ $Cs_2AgBi_{0.75}Sb_{0.25}Br_6$/ZnO (Fig. 2 and Table 2).

Fig. 3a shows the SEM image of ZnO nanoplate synthesized via the hydrothermal method, which is used as ETM in perovskits solar cells. This morphology indicates a high surface area-to-volume ratio, which is beneficial for electron transfer and interface contact. The ZnO plates appear well-aligned and densely packed,

Table 3. Impact of Cu_2O layer thickness on solar cells

Thickness(μm)	$V_{oc}(V)$	$J_{sc}(mA/cm^2)$	F.F (%)	η (%)
0.1	1.3478	13.817631	48.30	9.00
0.15	1.3478	13.825879	48.30	9.00
0.2	1.3478	13.832739	48.29	9.00
0.25	1.3478	13.838478	48.28	9.01
0.3	1.3478	13.843305	48.28	9.01
0.35	1.3478	13.847385	48.27	9.01
0.4	1.3478	13.850850	48.27	9.01
0.45	1.3478	13.853805	48.27	9.01
0.5	1.3478	13.856336	48.27	9.01
0.55	1.3478	13.858513	48.26	9.02
0.6	1.3478	13.860392	48.26	9.02
0.65	1.3478	13.862020	48.26	9.02
0.7	1.3478	13.863436	48.26	9.02

Table 4. Range of thickness for $Cs_2AgBi_{0.75}Sb_{0.25}Br_6$ with device parameters.

Thickness(μm)	$V_{oc}(V)$	$J_{sc}(mA/cm^2)$	F.F (%)	η (%)
0.1	1.3666	23.825909	49.84	16.23
0.2	1.3510	16.314075	46.65	10.28
0.3	1.3483	14.211780	47.96	9.19
0.4	1.3478	13.85813	48.26	9.02
0.5	1.3478	13.805578	48.31	8.99
0.6	1.3478	13.801354	48.31	8.99
0.7	1.3478	13.804692	48.31	8.99
0.8	1.3478	13.808875	48.30	8.99
0.9	1.3478	13.812852	48.29	8.99
1	1.3478	13.816503	48.29	8.99

which can improve charge mobility and reduce recombination losses in devices. The SEM image in Fig. 3b reveals a dense and uniform distribution of Cu_2O nanoparticles with roughly cubic or slightly rounded morphology. The particles appear to be nanometer-sized, in the range of 20–100 nm. Cu_2O

Table 5. Changes of thickness for ZnO with device parameters.

Thickness(μm)	$V_{oc}(V)$	$J_{sc}(mA/cm^2)$	F.F (%)	η (%)
0.01	1.3668	24.916751	41.04	13.98
0.02	1.3667	24.510749	42.32	14.18
0.03	1.3667	24.188570	45.22	14.95
0.04	1.3666	23.960753	48.03	15.73
0.05	1.3666	23.825909	49.84	16.23
0.06	1.3665	23.773931	50.77	16.49
0.07	1.3665	23.790783	51.08	16.61
0.08	1.3665	23.861225	51.05	16.64
0.09	1.3664	23.966513	50.84	16.65
0.1	1.3664	24.066006	50.61	16.64
0.2	1.3661	24.008441	50.35	16.51
0.3	1.3660	23.901613	50.31	16.42
0.4	1.3658	23.829946	50.28	16.36
0.5	1.3658	23.780783	50.26	16.32
0.6	1.3657	23.746324	50.24	16.29
0.7	1.3657	23.721682	50.23	16.27

Table 6. Coefficient for $Cu_2O/Cs_2AgBi_{0.75}Sb_{0.25}Br_6$/ZnO heterojunction solar cells.

Temperature(K)	$V_{oc}(V)$	Jsc (mA/cm^2)	F.F (%)	η (%)
100	1.1818	23.875135	59.15	16.69
150	1.3461	23.888415	53.30	17.14
200	1.3461	23.888415	53.30	17.14
250	1.3461	23.888415	53.30	17.14
300	1.4250	23.794833	50.66	17.18
350	1.3461	23.888415	53.30	17.14
400	1.2650	23.902571	56.14	16.98
450	1.1818	23.875135	59.15	16.69
500	1.0964	23.833503	61.82	16.15

ess on solar cells

nanoparticles are used as a hole transport layer in perovskite solar cells. This topography promotes efficient hole extraction and transport, while suppress electron recombination and ensure good interfacial contact with the perovskite absorber layer.

RESULTS AND DISCUSSION

Impact of Cu_2O layer thickness on solar cells

To maximize photon absorption and electron-hole pair generation, the absorber layer's thickness must be fine-tuned. In the past, active layer dimension has varied between 0.1 and 0.7 µm. Light with a longer wavelength induces a good rate of generation of electron-hole pairs in absorber layer. Increasing the thickness of the absorber layer brings the depletion layer closer to the back contact, allowing the back contact to catch more electrons for recombination [25]. The relationship between absorber layer thickness and PV parameter variation is shown in Fig. 4. Filling factor, current density, voltage density, and efficiency all raise with increasing thickness. At a thickness of 0.55 µm, the efficiency hits 9.02, allowing it to achieve peak performance. The statistics from the drawings are displayed in Table 3.

Impact of $Cs_2AgBi_{0.75}Sb_{0.25}Br_6$ layer thickness change on solar cells

This research looks at a PV design that uses a perovskite absorber material that is lead free and analyzes it using computer modeling tools. The energy bandgap of this novel structure is 1.80 eV, and it is made of a cesium-based double perovskite material [20-23]. The desirable characteristics displayed by the $Cs_2AgBi_{0.75}Sb_{0.25}Br_6$ are well-aligned bandgaps and increased stability under room temperature. A solar cell's efficiency is highly dependent on the thickness of its absorber layer. In terms of absorber layer thickness, $Cs_2AgBi_{0.75}Sb_{0.25}Br_6$ has varied between 0.1 µm

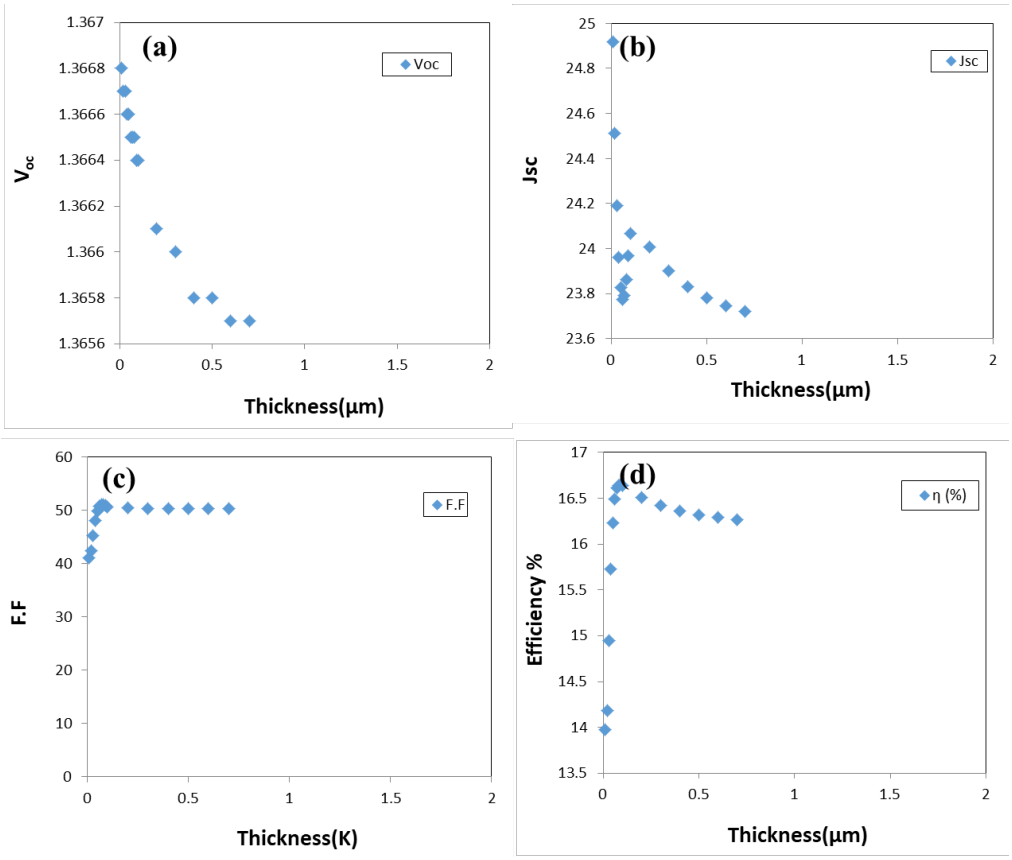

Fig. 6. The range of possibilities of (a) V_{oc}, (b) J_{sc}, (c) F.F, and (d) Efficiency with different thicknesses of ZnO.

and 1 µm. Fig. 5 shows how the photovoltaic properties of perovskite change with thickness. At 0.5 µm and 1 µm, the efficiency is 8.99 %. At 0.4 µm, efficiency rises to 9.02%, and at 0.3 µm, it remains constant almost. The optimal thickness for a solar cell is 0.1 µm, where the efficiency is 16.2%. Reduction in absorber layer thickness result in an enhancement in the number of electrons caught for recombination, making the depletion layer compatible with the back contact (Table 4). Observing the graphs of F.F/thickness, Voc/thickness, and Jsc/thickness, it is possible to observe that the FF value increases at a thickness of 0.1 µm, while Voc remains constant. Lastly, the value of Jsc grows as the thickness decreases.

Impact of ZnO layer thickness change on solar cells

Fig. 6 exhibits a findings of the research in which we projected the effect of increasing thickness of ZnO from 0.01 µm to 0.7 µm. A reduction in productivity can be observed as the dimension of the ZnO layer is increased; specifically, the efficiency value reaches its peak at 0.08 µm, which is 16.64%. This is due to the fact that a larger amount of radiation is absorbed, leading to the generation of a large number of excitons (Table 5). The value of the energy gap also plays a role in this equation [15, 17]. For example, when the material's energy gap is minimal and its wavelength is close to that of red light, the number of excitons increases and the efficiency rises. While Voc drops from 1.3668 V to 1.3657 V as the thickness increases from 0.01 µm to 0.7 µm. The Jsc drops from 24.916751 to 23.966513 mA/cm^2 as the thickness increases from 0.01 µm to 0.09 µm. The fill factor (FF) gets from 41.04% to 50.24% as the thickness increases from 0.01 µm to 0.7 µm.

Effect of annealing Temperatures for $Cs_2AgBi_{0.75}Sb_{0.25}Br_6$

We find that a temperature of 300 K, J_{sc} = 23.794833 (mA/cm^2), FF = 50.66%, and V_{oc} =

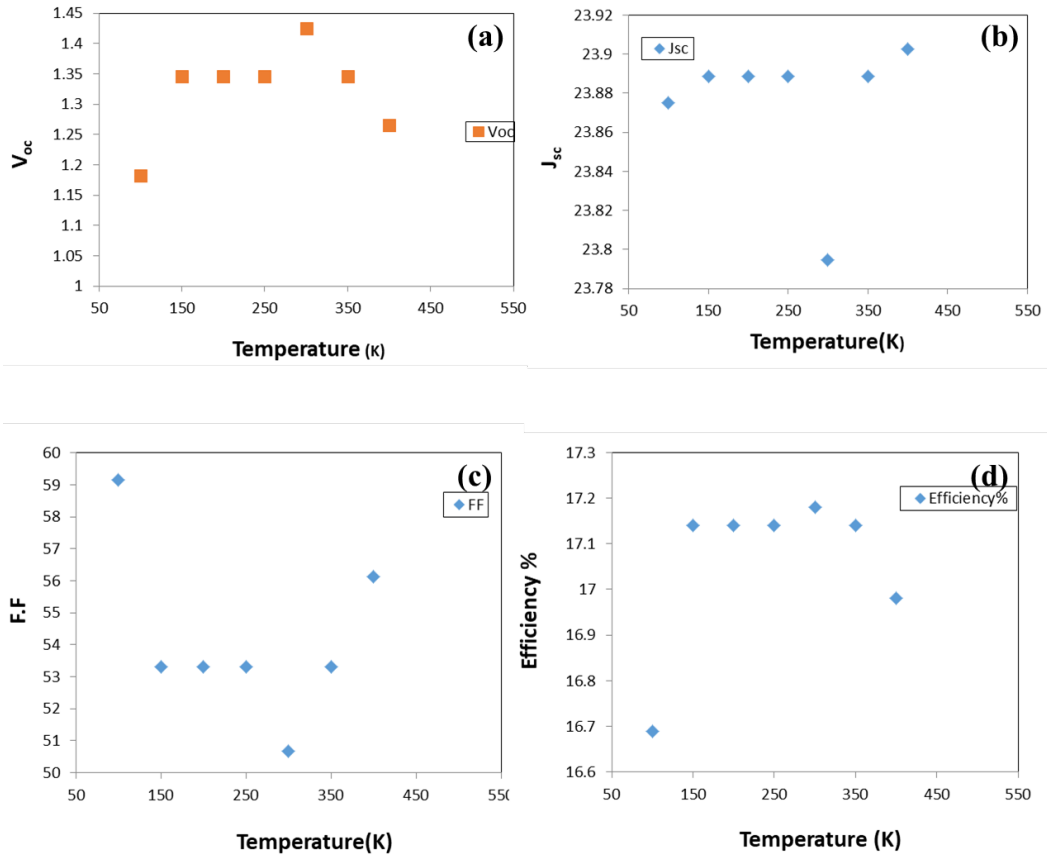

Fig. 7. The range of possibilities of (a) Voc, (b) Jsc, (c) F.F, and (d) Efficiency as a reflection of temperature for solar cells.

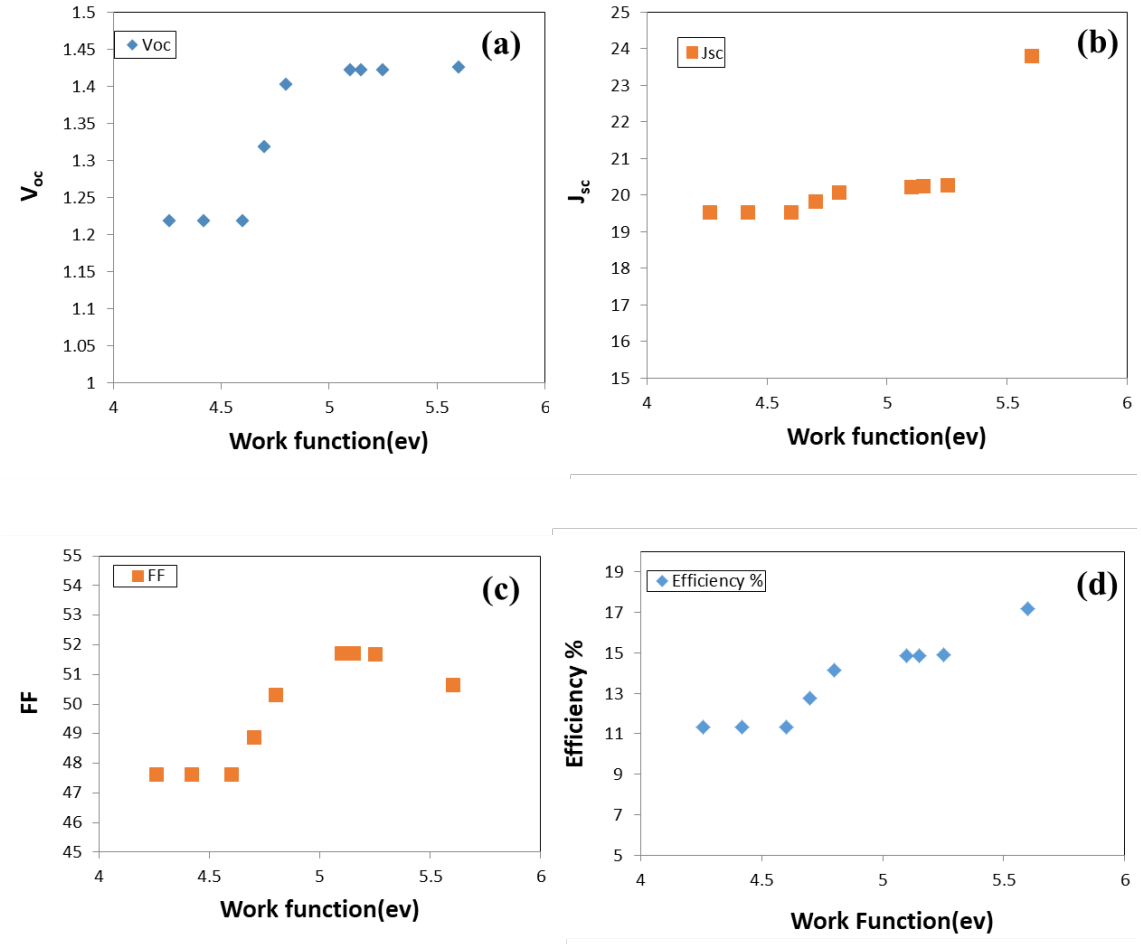

Fig. 8. The range of possibilities of (a) Voc, (b) Jsc, (c) F.F, and (d) Efficiency in relation to the functional unit of work.

Table 7. Impact of different metal contacts on the cell's efficiency.

Metals	Work Function (ev)	V_{oc}(V)	J_{sc}(mA/cm^2)	F.F (%)	Efficiency%
Al	4.26	1.2185	19.546135	47.64	11.35
Sn	4.42	1.2185	19.546135	47.64	11.35
Cu	4.6	1.2185	19.546134	47.64	11.35
Ag	4.7	1.3180	19.826673	48.88	12.77
Fe	4.8	1.4021	20.070282	50.33	14.16
Au	5.1	1.4217	20.235074	51.71	14.88
Ni	5.15	1.4217	20.246817	51.71	14.88
Ir	5.25	1.4218	20.279651	51.70	14.91
Pt	5.6	1.4250	23.794833	50.66	17.18

1.4250 as model's optimal operating conditions yield an efficiency value of 17.18%. An important factor influencing output is the ambient temperature. As demonstrated in Fig. 7, the PCE, FF, V_{oc}, and J_{sc} all climb from 100 K to 250 K as a result of an enhancement on formation of hole-electron in the perovskite materials. However, when the temperature increases to 300 K, J_{sc} (mA/cm^2) and FF decrease. The appropriateness temperature for using perovskites solar cells with $Cs_2AgBi_{0.75}Sb_{0.25}Br_6$ as a PVSC is 300 k, as we can see in Table 6. The device performance can be changed with temperature changes due to the ability for controlling the recombination, creating charge carriers, and so on.

Impact of various back contact materials

Two major obstacles to the widespread usage of perovskite solar cells are their expensive price and the fact that their back contact is thermally unstable. Based on Table 7, we used a many value for (Back) work function from 4.26 to 5.6 eV to get a back connection with higher specs. Fig. 8 shows that as the work function material increases, the values of Voc (1.2185 V to 1.4250 V), Jsc (19.546135 mA/cm^2 to 23.794833 mA/cm^2), Filling factor (47.64% for 50.66%), and η (11.35% to 17.18%) also rise. The parameters increaces as the work function (back contact) rises, which is related to the reduced Schottky barrier at the Cu_2O-contact interface.

CONCLUSION

This study comprehensively examines a revolutionary lead-free perovskite solar cell based on $Cs_2AgBi_{0.75}Sb_{0.25}Br_6$. A standard configuration of FTO/Cu_2O/ $Cs_2AgBi_{0.75}Sb_{0.25}Br_6$/ZnO/Pt was computed and examined utilizing SCAPS-1D simulation software. The influence of absorber layer on device performance was analyzed to achieve optimal efficiency. Result has shown that a perovskite solar cell utilizing $Cs_2AgBi_{0.75}Sb_{0.25}Br_6$ exhibits superior performance due to its optimal band alignment with the electron transport layer and hole transport layer. Additionally, the photovoltaic efficiency of the cell has been enhanced by adjusting three key parameters: temperature, work function, and absorber layer thickness. Our investigation elucidated the substantial impact of these three factors on the electrical characteristics of the PSC. The findings indicated that the ideal thickness of the light absorber was 1.5 µm and the optimal temperature was 300 K. Minimizing the absorber layer thickness markedly improves the PCE, achieving a result of about 16.23%. Our innovative findings may offer a feasible approach to produce economical, highly efficient, and stable $Cs_2AgBi_{0.75}Sb_{0.25}Br_6$-based perovskites.

CONFLICT OF INTEREST

The authors declare that there is no conflict of interests regarding the publication of this manuscript.

REFERENCES

1. Raheem Z, Zainab RA, Sally Basim K, Samir MA, Hayder Saadoon A. High Efficiency (22.46) of Solar Cells Based on Perovskites. University of Thi-Qar Journal of Science. 2023;10(2):187-191.
2. Zainab RA, Samir MA. High Efficiency Solar Cells Base on Organic-inorganic Perovskites Materials. University of Thi-Qar Journal of Science. 2021;8(2):23-29.
3. Enhancement Efficiency of Active Layer P3HT:POT:DBSA/PCBM Photoactive Solar Cell Device. University of Thi-Qar Journal of Science. 2020:90-94.
4. Miller OD, Yablonovitch E. Photon extraction: the key physics for approaching solar cell efficiency limits. SPIE Proceedings; 2013/09/11: SPIE; 2013. p. 880807.
5. Highest Efficiency of Perovskite Structure Solar Cells. International Journal of Thin Film Science and Technology. 2024;13(1):37-45.
6. Hadi S, Al-Khursan AH. Recombination rates of the double quantum dot solar cell structure. Phys Scr. 2021;96(12):125820.
7. Khadier HM, Al Husseini HB, Jafar AM. An Analysis Comparing The Performance Of Lead And Tin Halides In Organic Perovskite Materials CH_3NH_3 $Pb_xSn_{1-x}I_3$, Where x = 1, 0.5, or 0, For Use In Solar Cells. Journal of Optics. 2024.
8. Dang Y, Zhou Y, Liu X, Ju D, Xia S, Xia H, et al. Formation of Hybrid Perovskite Tin Iodide Single Crystals by Top-Seeded Solution Growth. Angew Chem Int Ed. 2016;55(10):3447-3450.
9. Zhou Y, Zhou Z, Chen M, Zong Y, Huang J, Pang S, et al. Doping and alloying for improved perovskite solar cells. Journal of Materials Chemistry A. 2016;4(45):17623-17635.
10. Wang N, Zhou Y, Ju MG, Garces HF, Ding T, Pang S, et al. Heterojunction-Depleted Lead-Free Perovskite Solar Cells with Coarse-Grained B-γ-$CsSnI_3$ Thin Films. Advanced Energy Materials. 2016;6(24).
11. Marshall KP, Walker M, Walton RI, Hatton RA. Enhanced stability and efficiency in hole-transport-layer-free CsSnI3 perovskite photovoltaics. Nature Energy. 2016;1(12).
12. Li B, Di H, Chang B, Yin R, Fu L, Zhang YN, et al. Efficient Passivation Strategy on Sn Related Defects for High Performance All-Inorganic $CsSnI_3$ Perovskite Solar Cells. Adv Funct Mater. 2021;31(11).
13. Ye T, Wang X, Wang K, Ma S, Yang D, Hou Y, et al. Localized Electron Density Engineering for Stabilized B-γ $CsSnI_3$-Based Perovskite Solar Cells with Efficiencies >10%. ACS Energy Letters. 2021:1480-1489.
14. Forgács D, Gil-Escrig L, Pérez-Del-Rey D, Momblona C,

Werner J, Niesen B, et al. Efficient Monolithic Perovskite/Perovskite Tandem Solar Cells. Advanced Energy Materials. 2016;7(8).
15. Cs_2AgBiX_6 (X = Br, Cl): New Visible Light Absorbing, Lead-Free Halide Perovskite Semiconductors. American Chemical Society (ACS).
16. Madan J, Shivani, Pandey R, Sharma R. Device simulation of 17.3% efficient lead-free all-perovskite tandem solar cell. Solar Energy. 2020;197:212-221.
17. Chen M, Ju M-G, Garces HF, Carl AD, Ono LK, Hawash Z, et al. Highly stable and efficient all-inorganic lead-free perovskite solar cells with native-oxide passivation. Nature Communications. 2019;10(1).
18. Abdulsada ZR, Abdul Almohsin SM. High Efficiency (9.60) of CI Perovskites base solar cells with PCBM (ETM) and P3HT(HTM). Journal of Physics: Conference Series. 2021;1999(1):012049.
19. Deng W, Fang H, Jin X, Zhang X, Zhang X, Jie J. Organic–inorganic hybrid perovskite quantum dots for light-emitting diodes. Journal of Materials Chemistry C. 2018;6(18):4831-4841.
20. Introducing Cu_2O Thin Films as a Hole-Transport Layer in Efficient Planar Perovskite Solar Cell Structures. American Chemical Society (ACS).
21. Amri K, Belghouthi R, Aillerie M, Gharbi R. Device Optimization of a Lead-Free Perovskite/Silicon Tandem Solar Cell with 24.4% Power Conversion Efficiency. Energies. 2021;14(12):3383.
22. M. AbdulAlmohsin S, E. Tareq D. Fabrication and simulation of peroviskite solar cells comparable study of CuO and Nano composite PANI/SWCNTS as HTM. AIMS Energy. 2020;8(2):169-178.
23. Jafar AM, Khalaph KA, Hmood AM, Abdalameera NK. Pb-Free metal halide double perovskite, Cs_2SbAgX_6, X = I or Cl, with TiO_2 nano-particles in solar cell applications. AIP Conference Proceedings: AIP Publishing; 2023. p. 090031.
24. mohammed khadier H, Al Husseini HB, Mashot Jafar A. An analysis comparing the performance of lead and tin halides organic Perovskite Solar Cells and numerical simulation with SCAPS. Opt Mater. 2024;155:115814.
25. Jafar AM, Al-Attar FM, Inad KI, Hmood AM, Saleh SM, Khalaph KA. Preparation and simulation of lead mix-halide perovskite solar cells. AIP Conference Proceedings: AIP Publishing; 2020.
26. Lian J, Lu B, Niu F, Zeng P, Zhan X. Electron-Transport Materials in Perovskite Solar Cells. Small Methods. 2018;2(10).
27. Jafar AM, Khalaph KA, Al Husseini HB. Study of the structural, electronic, mechanical, electro-thermal and optical properties of double perovskite structures Cs_2SbAgX_6, (X = I, Br, or Cl). Phys Scr. 2022;97(8):085509.
28. Shasti M, Mortezaali A. Numerical Study of Cu_2O, $SrCu_2O_2$, and $CuAlO_2$ as Hole-Transport Materials for Application in Perovskite Solar Cells. physica status solidi (a). 2019;216(18).